

Supplementary Information

The Unexpected Effect of Ferrocenyl Substituents on the Photochemistry of Dianthryl Sulfoxides

Nicole Removski and Michael O. Wolf*

Department of Chemistry, 2036 Main Mall, University of British Columbia, Vancouver, BC, V6T 1Z1, Canada

Experimental Details	S2
General.....	S2
Spectroscopy, Spectrometry & Crystallography.....	S2
Electrochemistry	S3
Synthetic Procedures	S3
Experimental Details.....	S3
9-Bromo-10-ferrocenylantracene.....	S3
1,1'-(Sulfinylbis(anthracene-10,9-diyl))diferrocene.....	S4
Structural Characterization.....	S5
Nuclear Magnetic Resonance.....	S5
Mass Spectrometry.....	S8
Crystallography.....	S21
Electrochemical Data.....	S25
Photochemical Data	S26
References	S28

Experimental Details

General

Starting materials were purchased from Strem Chemicals, VDW International Co., Thermo Fisher Scientific Chemicals Inc., Alfa Aesar, Sigma Aldrich, or AmBeed, Inc, and used without further purification other than ferrocene, which was sublimed under vacuum onto a cold finger. Potassium *tert*-butoxide was purified by dissolving in THF in an oven-dried Schlenk flask, transferring the supernatant to another flask under N₂ and evacuating solvent under vacuum in the Schlenk line. Unless otherwise stated, all experiments were carried out under a nitrogen atmosphere using standard Schlenk line techniques. Degassed, purified, and dry tetrahydrofuran (THF) was freshly obtained in an oven-dried Schlenk bomb from an Innovative Technology Inc. solvent purification system (SPS) for each reaction. Unless otherwise stated, all solvents were obtained commercially from Sigma-Aldrich. Column chromatography was carried out using silica gel (SilicaFlash ® F60, 230-400 mesh). The synthesis of 9-bromo-10-ferrocenylanthracene (**FcAnBr**) was adapted and optimized from the literature.

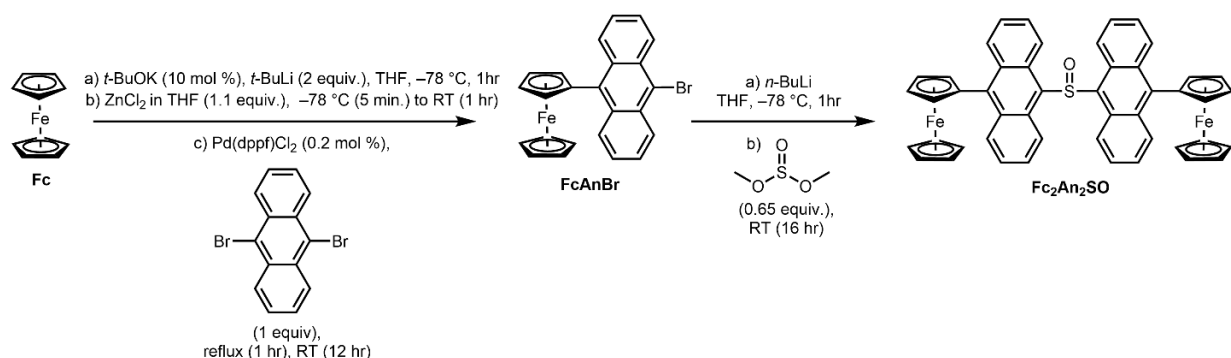
Spectroscopy, Spectrometry & Crystallography

¹H and ¹³C NMR spectra were recorded in deuterated chloroform (CDCl₃, CIL or AO) or deuterated dimethyl sulfoxide (DMSO-d₆, CIL) on a Bruker Avance 400 Hz inverse probe, Bruker Avance 300 Hz with autosampler, or Bruker Avance 600 Hz spectrometer, referenced to the residual protonated solvent peak. All samples for photophysical measurements were diluted ten-fold in volumetric flasks and transferred in a dark fume hood to a quartz cuvette with a path length of one centimetre. A Cary 5000 UV-Vis-NIR spectrophotometer was used for all absorption measurements and an Agilent Cary Eclipse fluorescence spectrometer was used to carry out all emission measurements. For the absorption scans, the scan was swept from 800 nm to 200 nm at a scan rate of 600 nm/min. To convert sulfoxide compounds to the associated photoproducts, a UV flashlight (254 nm, Entella) was pulsed at the edge of the cuvette containing the sample in between scans. Electron paramagnetic resonance (EPR) spectra were taken on a Bruker ELEXSYS E560 spectrometer equipped with a X-band microwave source (7.0–10 GHz). Low- and high-resolution mass spectra were collected on a AccuTOF™ GCx Gas Chromatograph equipped with a field desorption (FD) ion source. Some high-resolution mass spectra were collected on a Waters Micromass LCT a time-of-flight mass spectrometer equipped with an atmospheric pressure chemical ionization (APCI) ion source. Crystals were recrystallised *via* slow vapour diffusion using hexane and DCM. Crystallographic properties were measured on a Bruker APEX-II CCD diffractometer at 296 K and the data was processed with the Bruker SAINT software package. Their structures were solved using the Olex2 software with the SHELXL solver and refined with the SHELXT refinement package.¹

Electrochemistry

The electrochemical properties of the prepared compounds were measured using cyclic voltammetry (CV) on a Metrohm Autolab PGSTAT12 potentiostat. CV measurements were carried out at room temperature in an airtight, 3-necked glass electrochemical cell, fitted with a 7 mm² glassy carbon working electrode, a platinum mesh counter electrode, and a silver wire reference electrode in a single compartment. The working electrode was polished with 1.0, 0.3 and 0.05 μM alumina paste. Each electrode was rinsed with an aqueous 6 M HCl solution, water, and acetone, followed by gentle drying with a Kimwipe. A 0.124 M background electrolyte solution was prepared with triply recrystallized tetrabutylammonium tetrafluorophosphate (TBAPF₆) in dry, degassed dichloromethane (CH₂Cl₂) from the SPS and was used as the solvent for all CV experiments. The compound of interest was added to the electrolyte at a concentration of 0.61 mM. The scan rate applied was 100 mVs⁻¹ and the current was set at 10 μA. Measurements taken were compared against ferrocene as an external standard after the measurements, run under identical conditions.

Synthetic Procedures



Scheme S1. Synthetic pathway to **Fc₂An₂SO**

Experimental Details

9-Bromo-10-ferrocenylanthracene. Ferrocene (500 mg, 2.7 mmol, 1 equiv.) and potassium *tert*-butoxide (30 mg, 0.27 mmol, 0.1 equiv.) were purified and dried, then loaded into an oven-dried, 250 mL Schlenk flask equipped with a stir bar in a glovebox. Dry THF (20 mL) from the SPS was added *via* syringe transfer and the solution was cooled to -78 °C. Maintaining -78 °C, *tert*-butyl lithium (3.36 mL, 1.6 M in pentane, 5.4 mmol, 2 equiv.) was added dropwise, then stirred for 1 h. A zinc chloride solution in THF (2.7 mL, 1 M, 1.1 equiv.) was prepared in the glovebox and transferred into the reaction flask at -78 °C. After five minutes, the reaction flask was warmed to room temperature and stirred for 1 hour. The cap of the reaction flask was removed; 9,10-dibromoanthracene (903 mg, 2.7 mmol, 1 equiv.) and [1,1'-bis(diphenylphosphino)ferrocene]palladium(II) dichloride ([dppf]PdCl₂), 4 mg, 0.2 mol%) were

quickly added. The flask was equipped with a condenser, heated at reflux for 1 hour, then stirred overnight. The reaction was quenched with water (20 mL), extracted with DCM, dried over MgSO₄, and concentrated under vacuum. The crude material was dry loaded onto a silica gel column and eluted with 100% hexanes which recovered the starting material (AnBr₂) and the intended cross-coupled product (269 mg, 29 %) as a waxy bright red solid. R_f = 0.4 (hexanes). Note: If the product is left under vacuum, under air and/or exposed to light for more than 24 h, photooxidation is observed. It is recommended that this compound be kept in the dark under an inert atmosphere or used immediately to avoid this. ¹H NMR (400 MHz, CDCl₃): δ 4.26 (s, 5H), δ 4.63 (pseudo t, 2H), δ 4.80 (pseudo t, 2H), δ 7.48 (m, 2H), δ 7.57 (m, 2H), δ 8.59 (d, 2H), δ 9.14 (d, 2H). ¹³C{¹H} NMR (600 MHz, CDCl₃): δ 67.98, δ 69.95, δ 73.66, δ 84.08, δ 124.33, δ 126.74, δ 127.95, δ 128.21, δ 130.43, δ 131.55, δ 133.15. HR-FD MS: *m/z* calc'd for ¹²C₂₄¹H₁₇⁷⁹Br⁵⁶Fe: 439.98630; Found: 439.98626 [M]⁺.³

1,1'-(Sulfinylbis(anthracene-10,9-diyl))diferrocene. In an oven-dried 25 mL Schlenk flask, dried 9-bromo-10-ferrocenylanthracene (150 mg, 0.34 mmol, 1.0 equiv.) that was previously dried under rotary evaporation and stored under N₂ was dissolved in dry THF (10 mL) and cooled to -78 °C in an acetone/dry ice bath. Maintaining -78 °C, *n*-butyllithium (0.26 mL, 1.6 M in hexanes, 0.40 mmol, 1.2 equiv.) was syringed into the reaction flask dropwise and stirred for 1 h. After turning off all fumehood lights and wrapping the flask with aluminum foil, positive N₂ pressure was applied, and the septum was removed. Dimethyl sulfite (17. μL, 0.20 mmol, 0.6 equiv.) was immediately added with a micropipette and the reaction was capped and warmed to room temperature, stirring overnight. The crude material was loaded onto a silica gel plug neat and eluted with 100% hexanes, 50/50 hexanes/DCM, then 100% DCM. The solvent was removed *in vacuo* and the product was recovered as a dark red solid (106 mg, 40%). ¹H NMR (400 MHz, CDCl₃): δ 4.11 (s, 5H), δ 4.55 (pseudo t, 2H), δ 4.67 (pseudo t, 2H), δ 7.36 (m, 4H), δ 9.08 (d, J = 8.68 Hz, 2H), δ 9.27 (d, 2H). ¹³C{¹H} NMR (600 MHz, CDCl₃): δ 68.35, δ 69.95, δ 73.66, δ 84.08, δ 124.33, δ 126.74, δ 127.95, δ 128.21, δ 130.43, δ 131.55, δ 133.15. FD-HRMS: *m/z* calc'd for ¹²C₄₈¹H₃₄⁵⁶Fe₂¹⁶O³²S: 770.10292; Found: 770.10204 [M]⁺.

Structural Characterization

Nuclear Magnetic Resonance

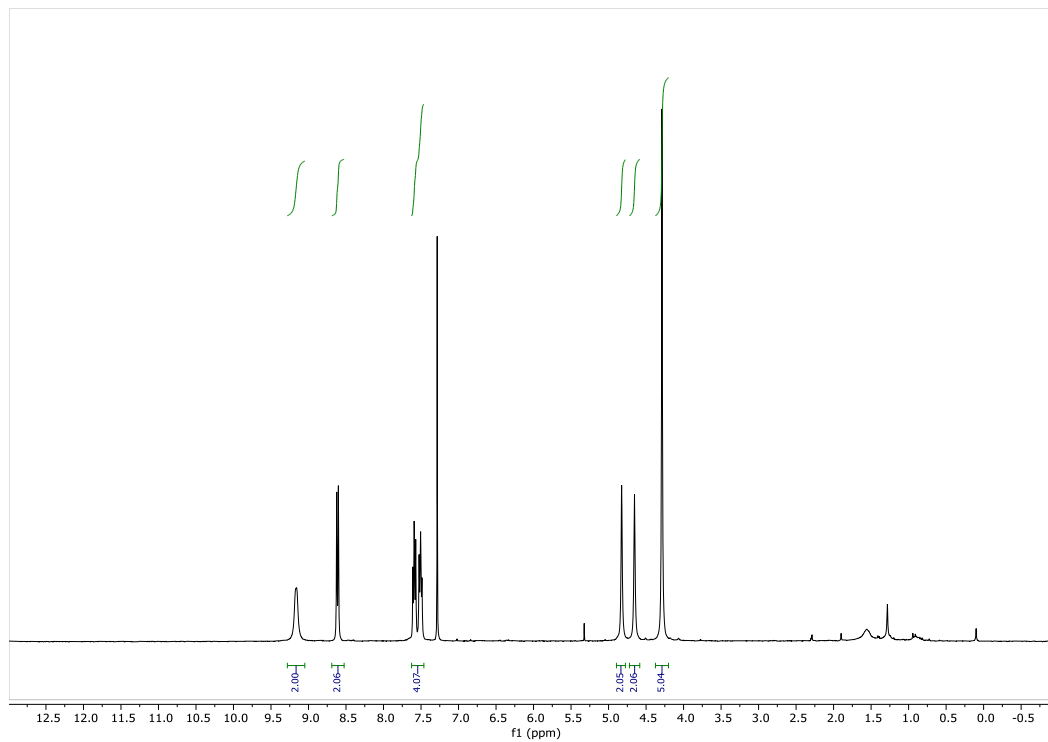


Figure S1. ^1H NMR spectrum of **FcAnBr** (CDCl_3 , 400 MHz, 25 °C).

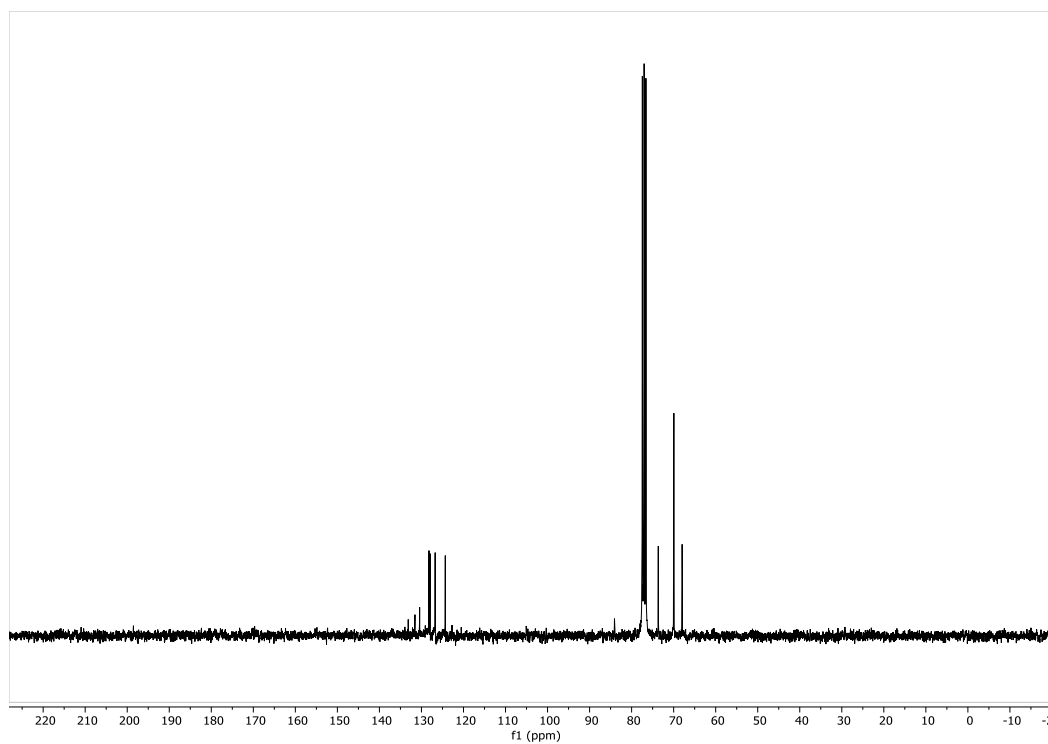


Figure S2. ^{13}C NMR spectrum of **FcAnBr** (CDCl_3 , 600 MHz, 25 °C).

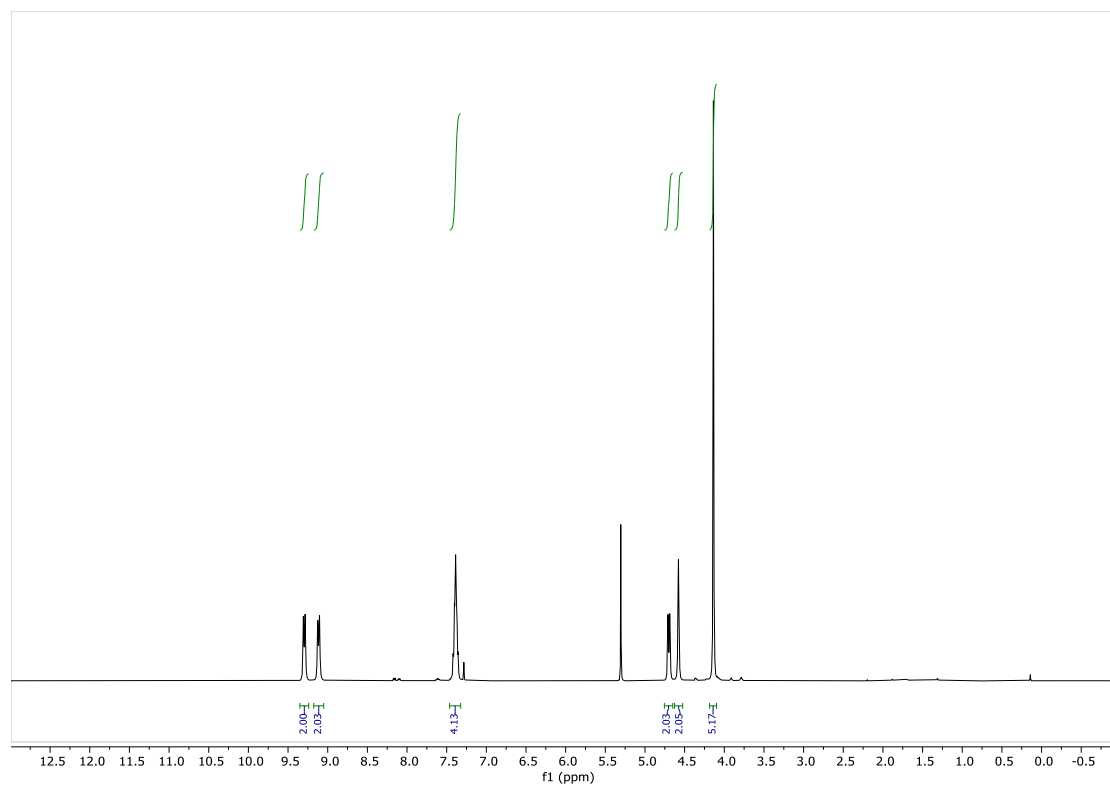


Figure S3. ^1H NMR spectrum of $\text{Fc}_2\text{An}_2\text{SO}$ (CDCl_3 , 400 MHz, 25 °C).

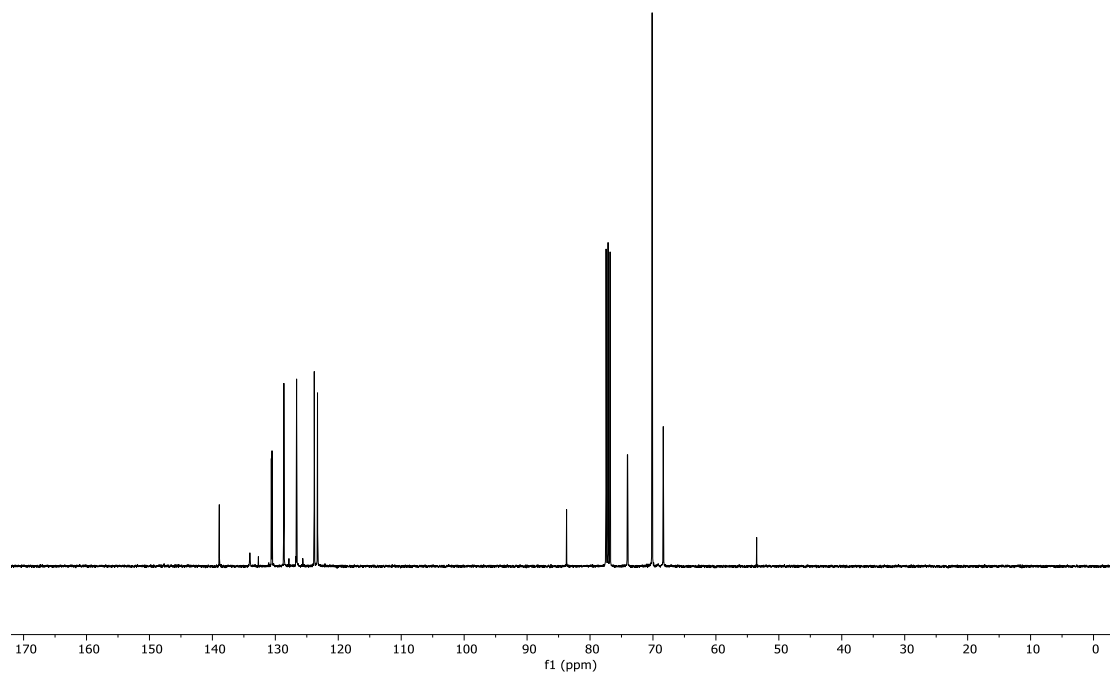


Figure S4. ^{13}C NMR spectrum of $\text{Fc}_2\text{An}_2\text{SO}$ (CDCl_3 , 600 MHz, 25 °C).

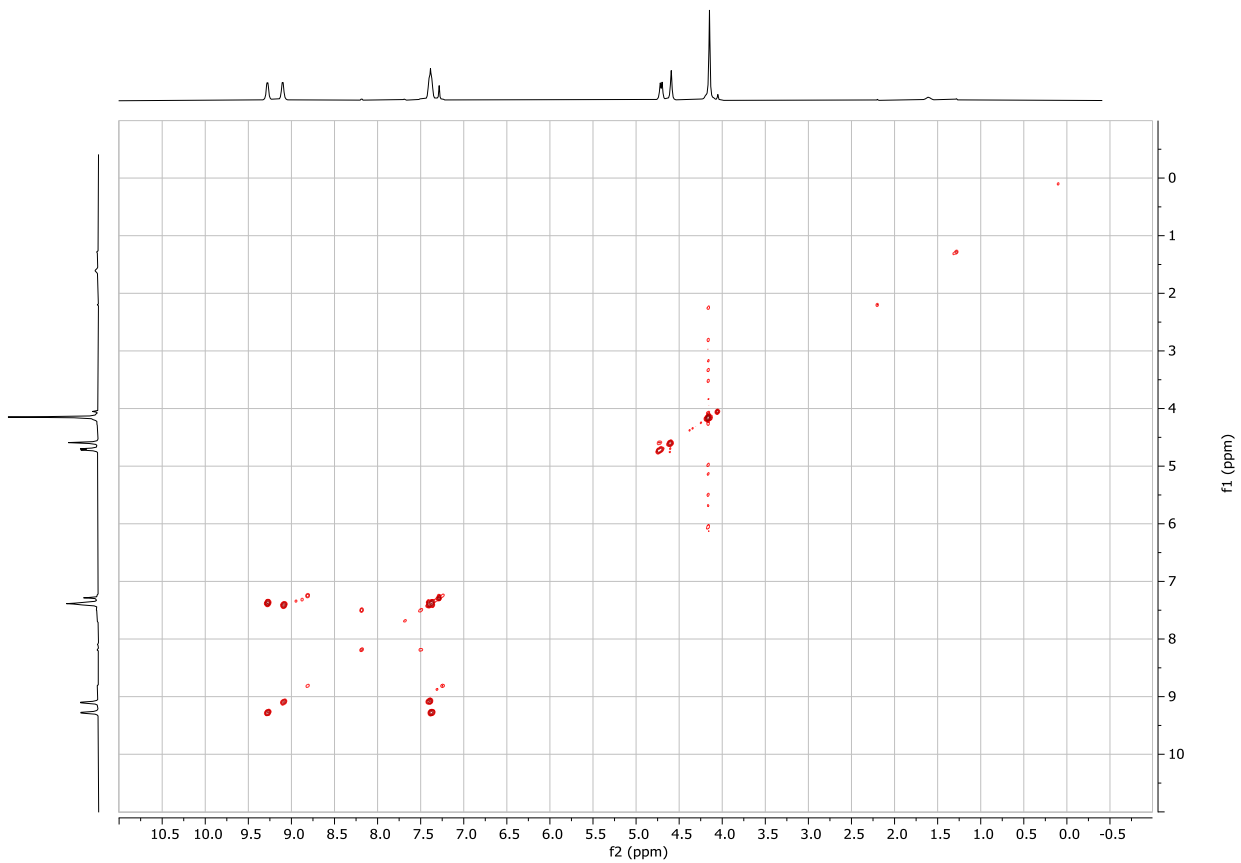


Figure S5. 2D COSY NMR spectrum of $\text{Fc}_2\text{An}_2\text{SO}$ (CDCl_3 , 600 MHz, 25 °C).

Mass Spectrometry

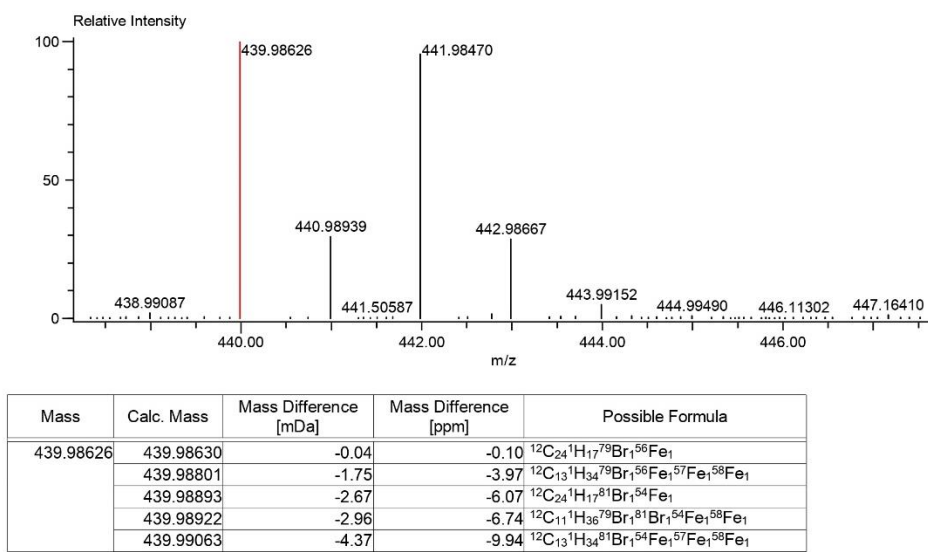


Figure S6. High Resolution FD-MS spectrum of **FcAnBr**.

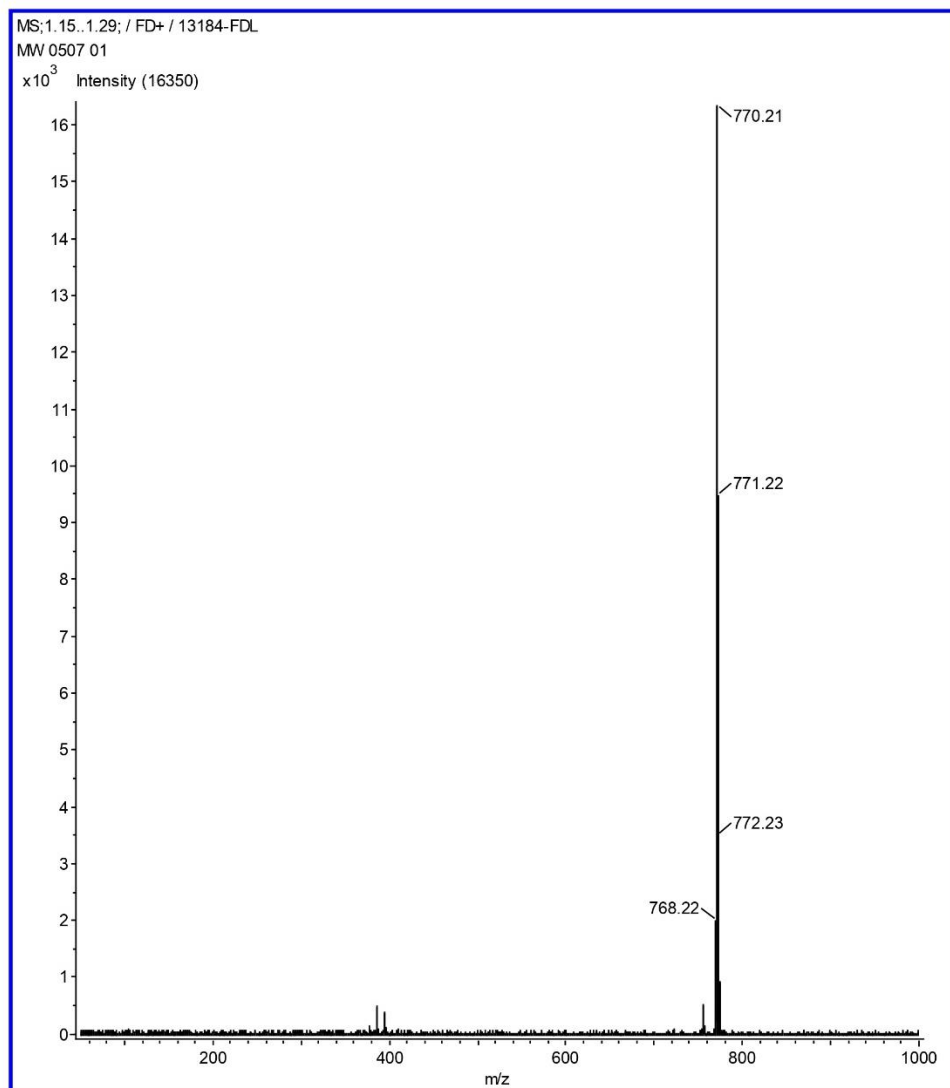


Figure S7. Low-resolution FD-MS spectra of **Fc₂An₂SO**.

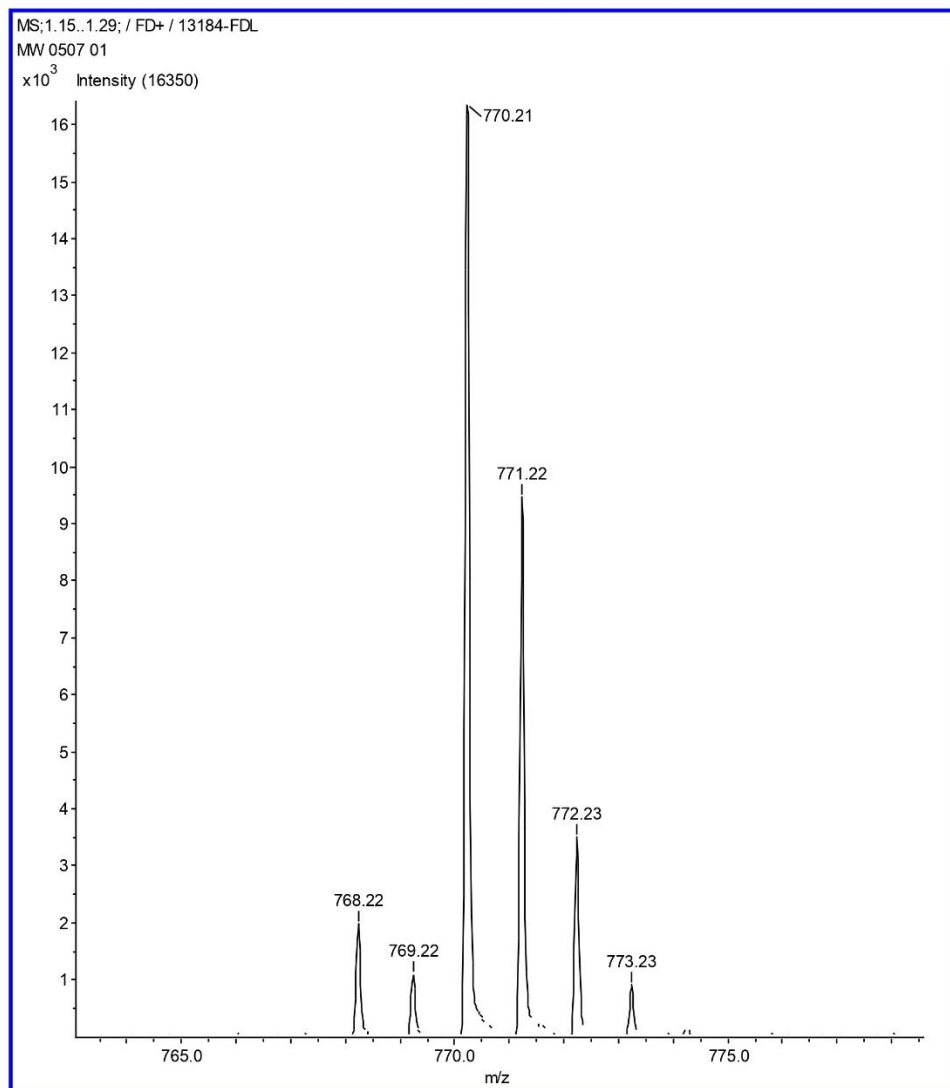


Figure S8. Low-resolution FD-MS spectra of **Fc₂An₂SO** (range from m/z = 765 to 775 shown).

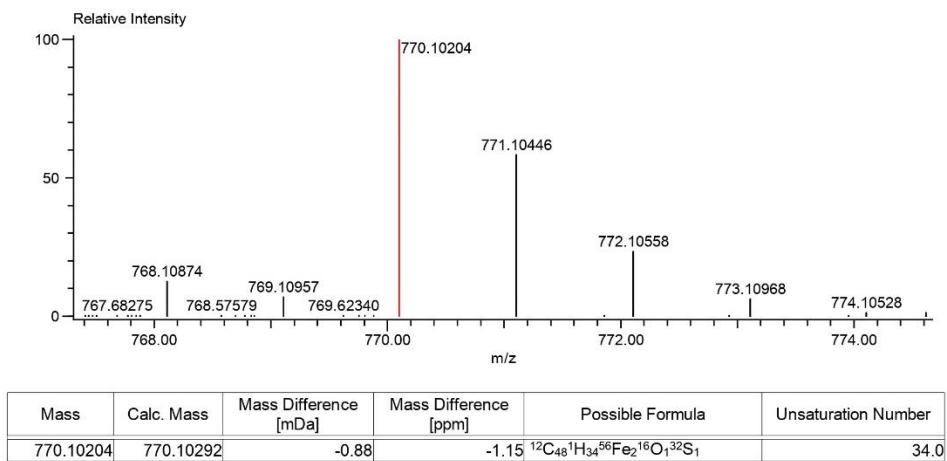


Figure S9. High-resolution FD-MS spectra of **Fc₂An₂SO**.

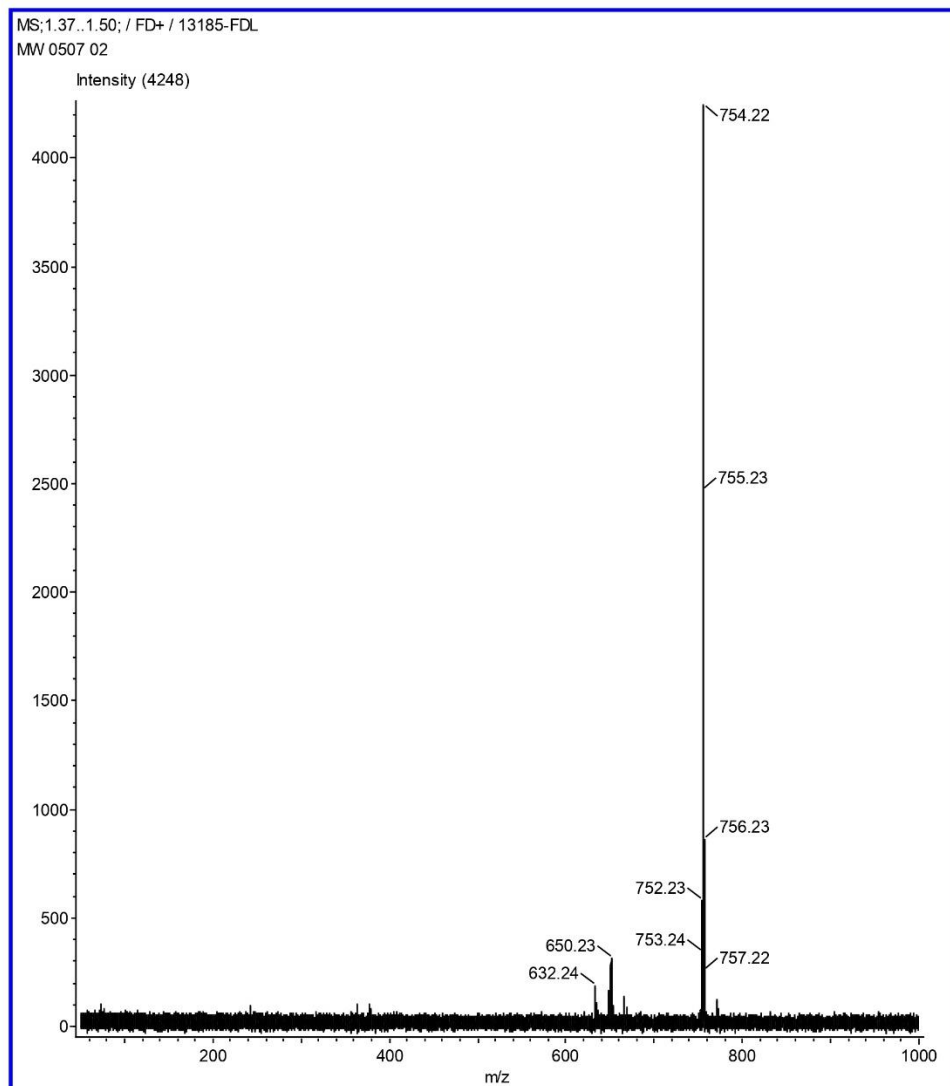


Figure S10. Low-resolution FD-MS spectra of irradiated $\text{Fc}_2\text{An}_2\text{SO}$.

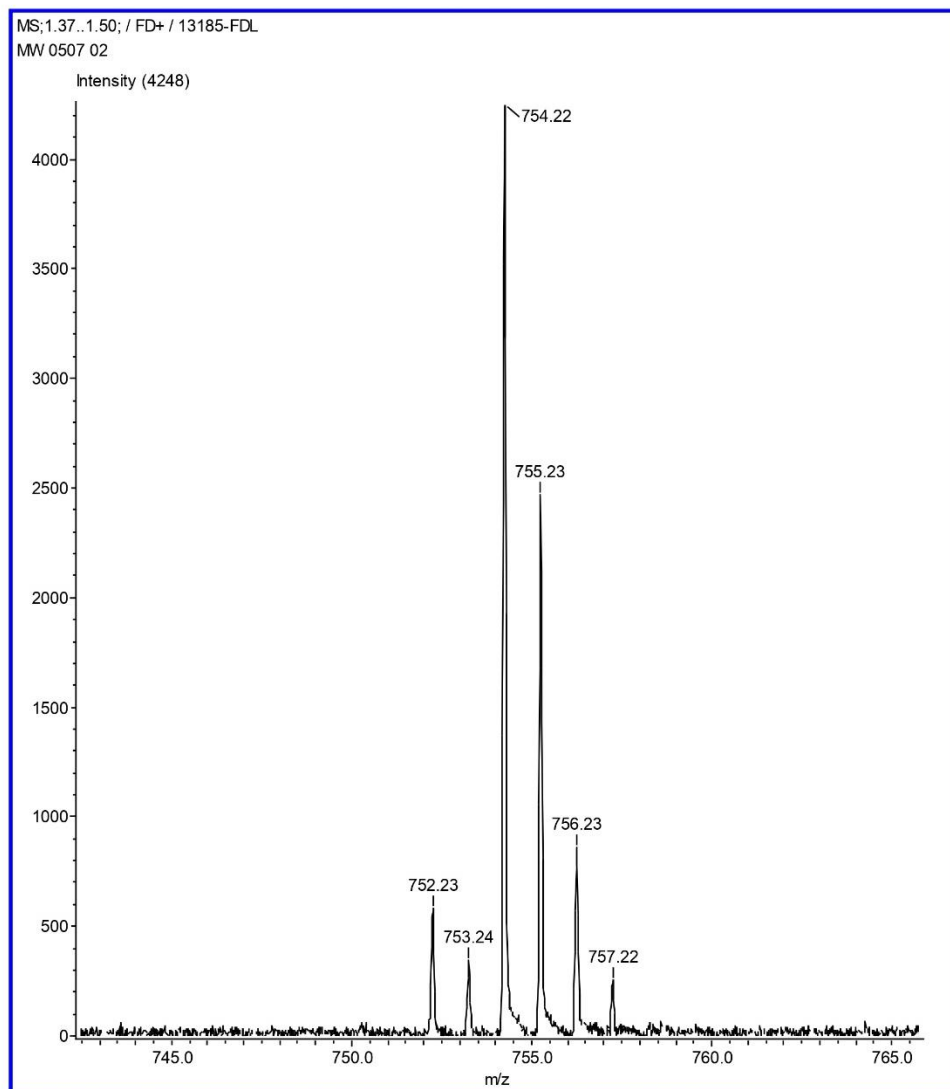


Figure S11. Low-resolution FD-MS spectra of irradiated $\text{Fc}_2\text{An}_2\text{SO}$ (range from $m/z = 745$ to 765 shown).

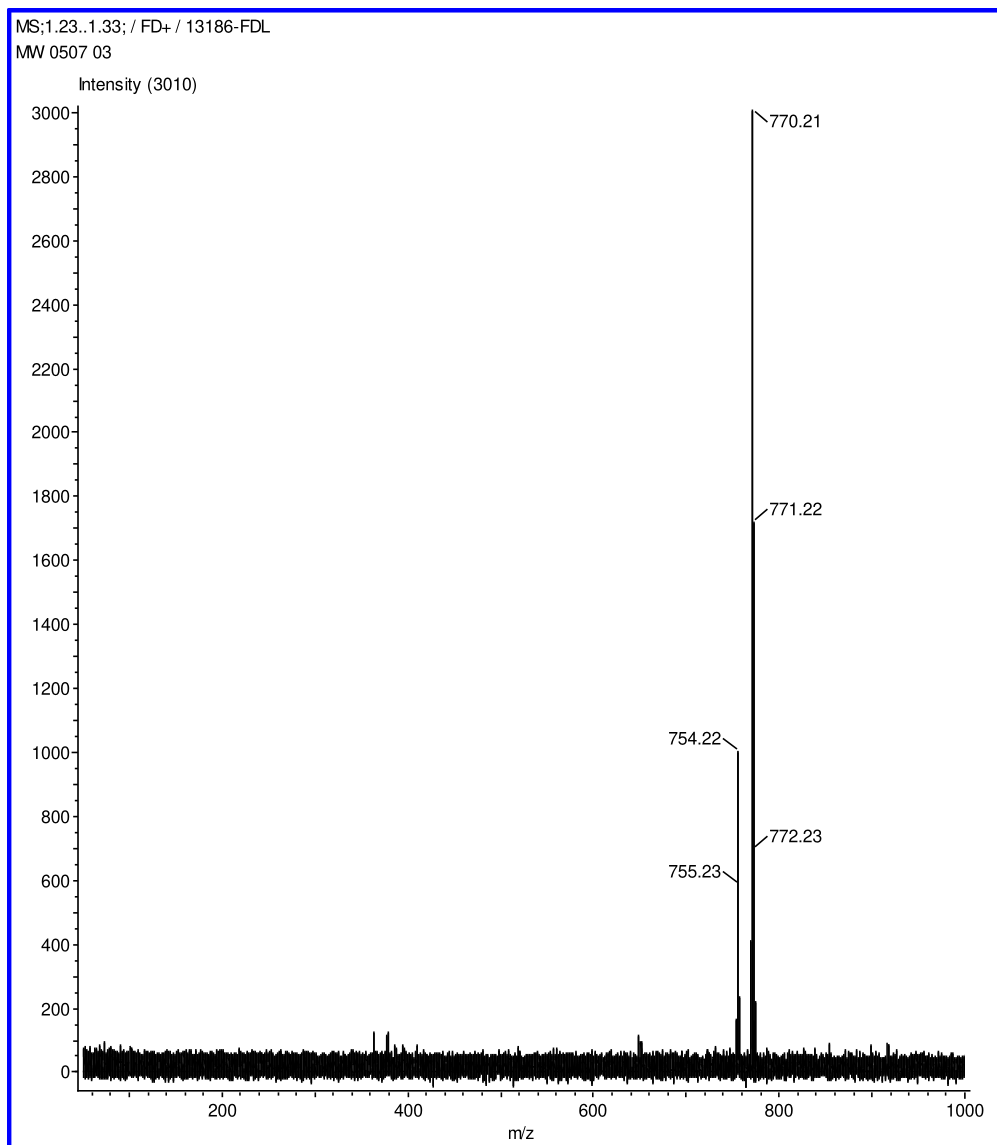


Figure S12. Low-resolution FD-MS spectra of chemically oxidized **Fc₂An₂SO**.

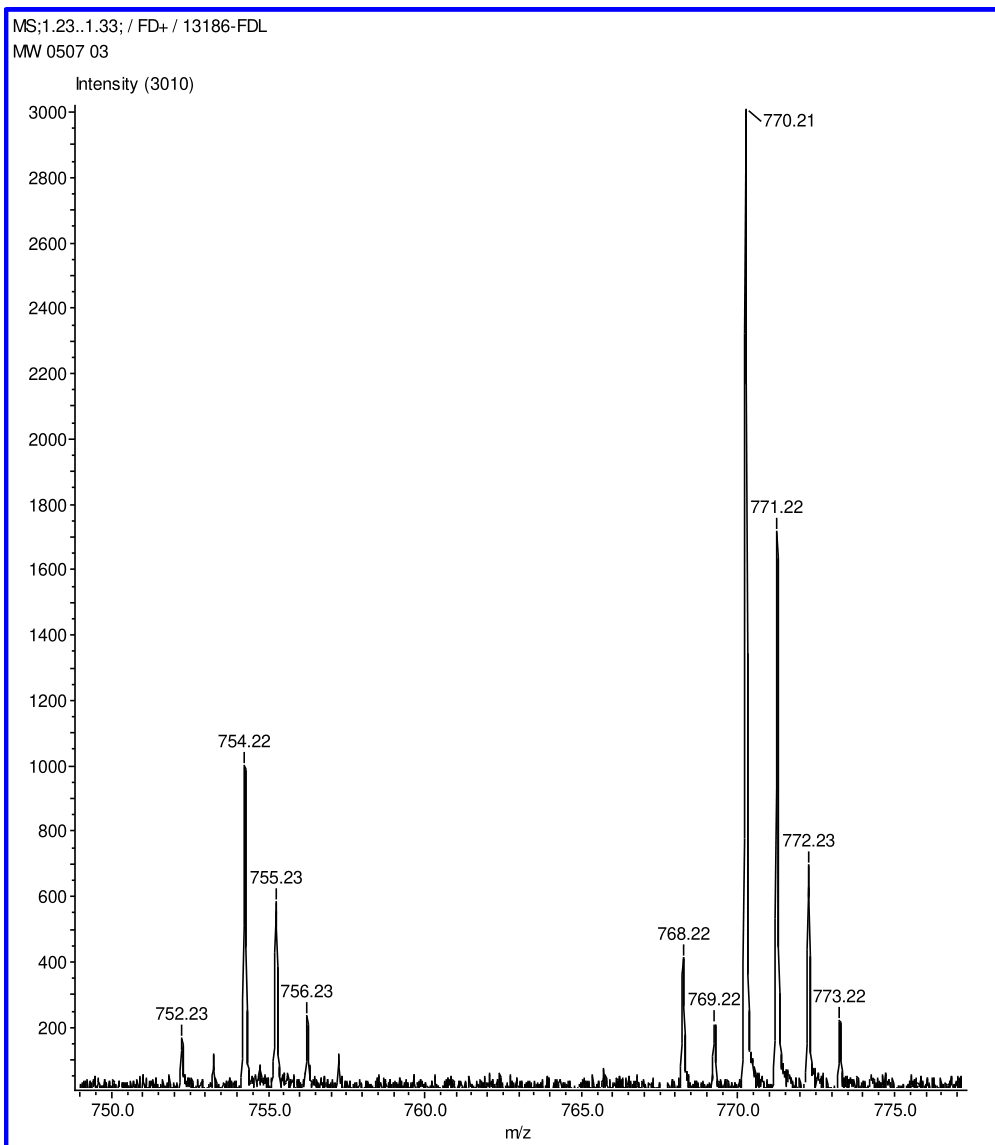
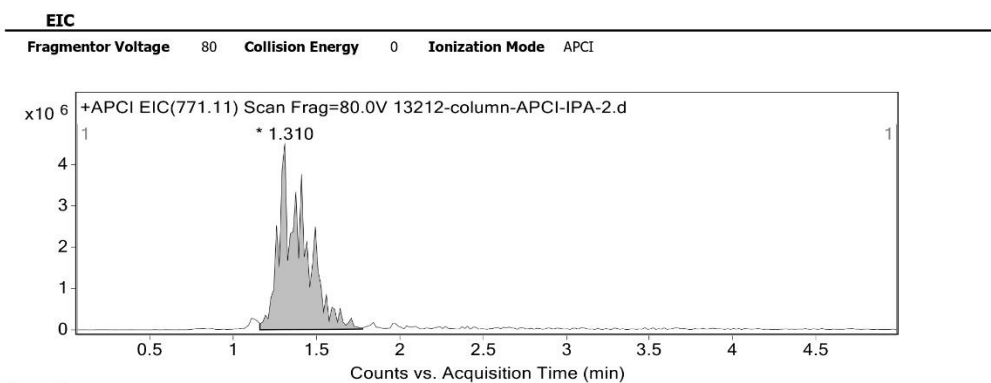


Figure S13. Low-resolution FD-MS spectra of chemically oxidized **Fc₂An₂SO** (range from $m/z = 750$ to 775 shown).

Chromatograms



Spectra

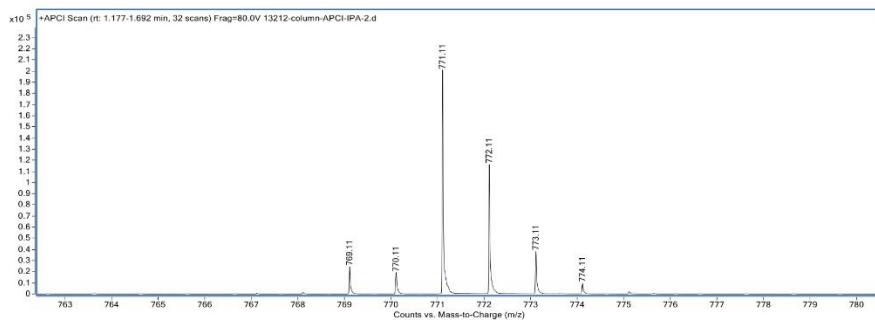
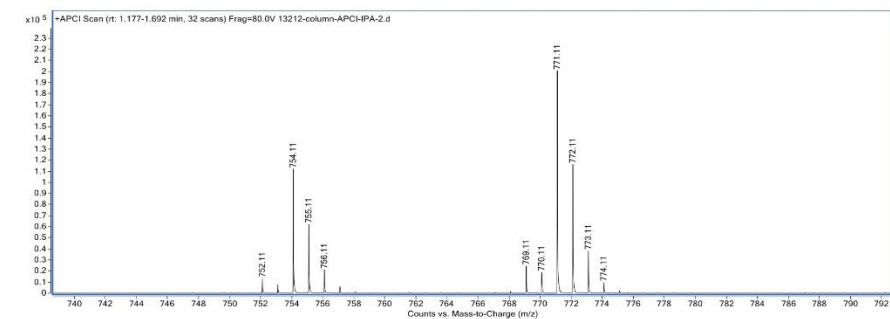
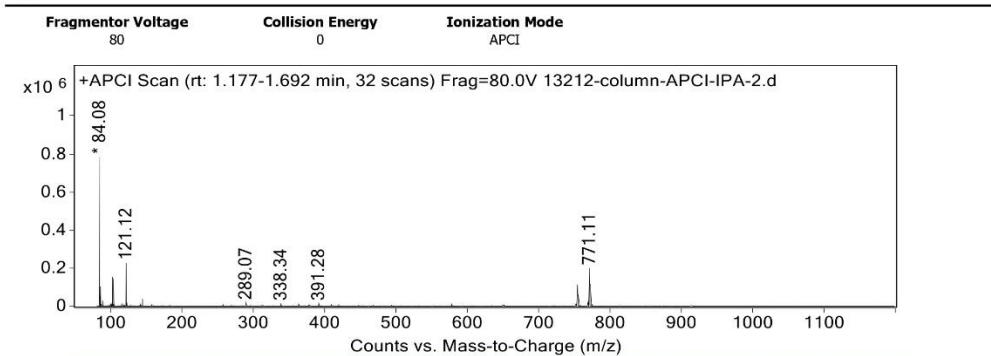


Figure S14. High-resolution APCI-MS spectra of chemically oxidized $\text{Fc}_2\text{An}_2\text{SO}$.

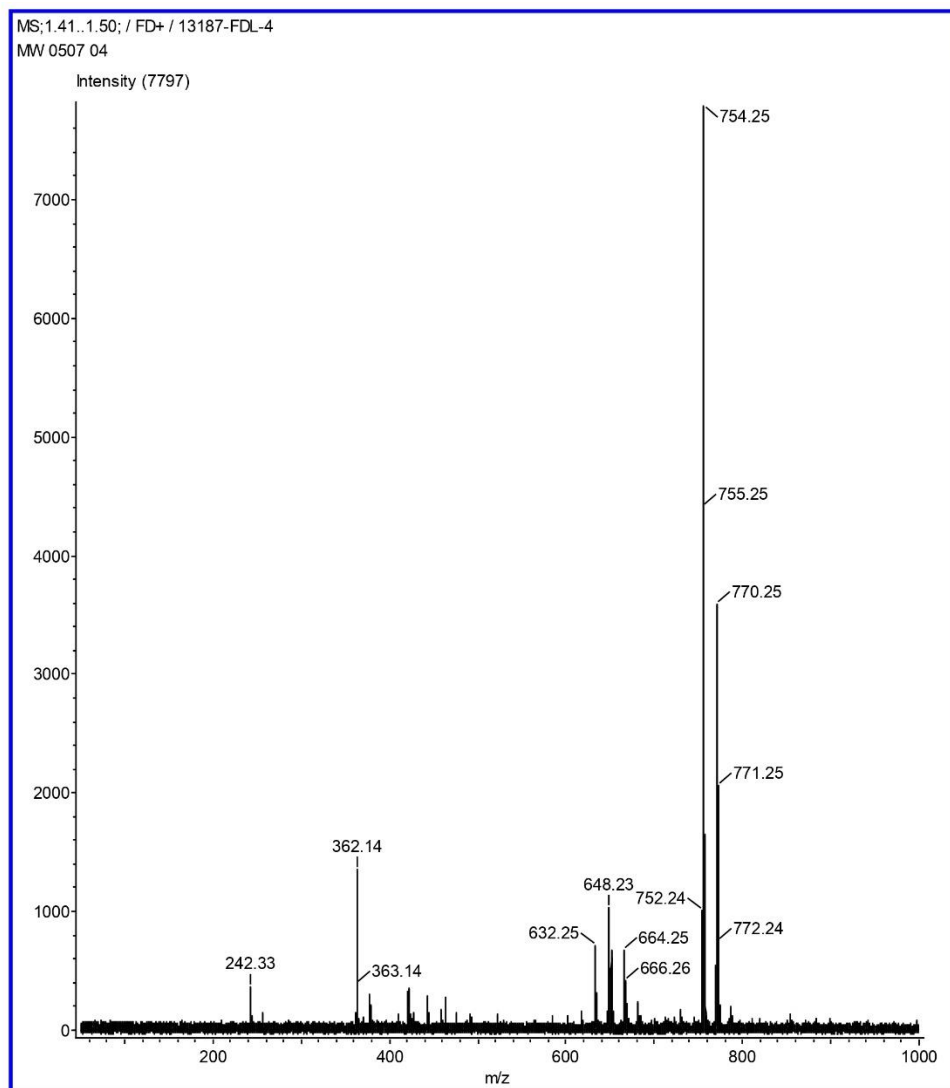


Figure S15. Low-resolution FD-MS spectra of chemically oxidized and irradiated $\text{Fc}_2\text{An}_2\text{SO}$.

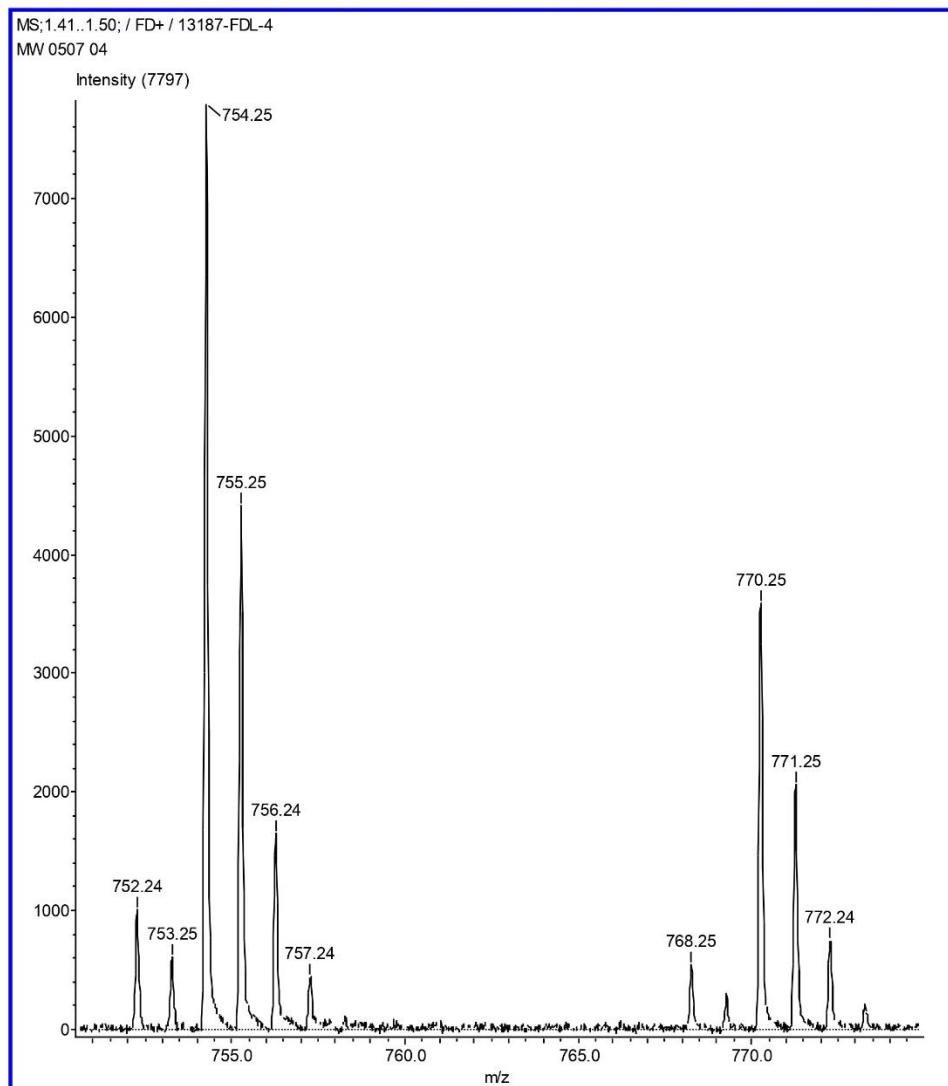


Figure S16. Low-resolution FD-MS & APCI-MS spectra of chemically oxidized, irradiated $\text{Fc}_2\text{An}_2\text{SO}$ (range from m/z 750 to 775 shown).

Spectra

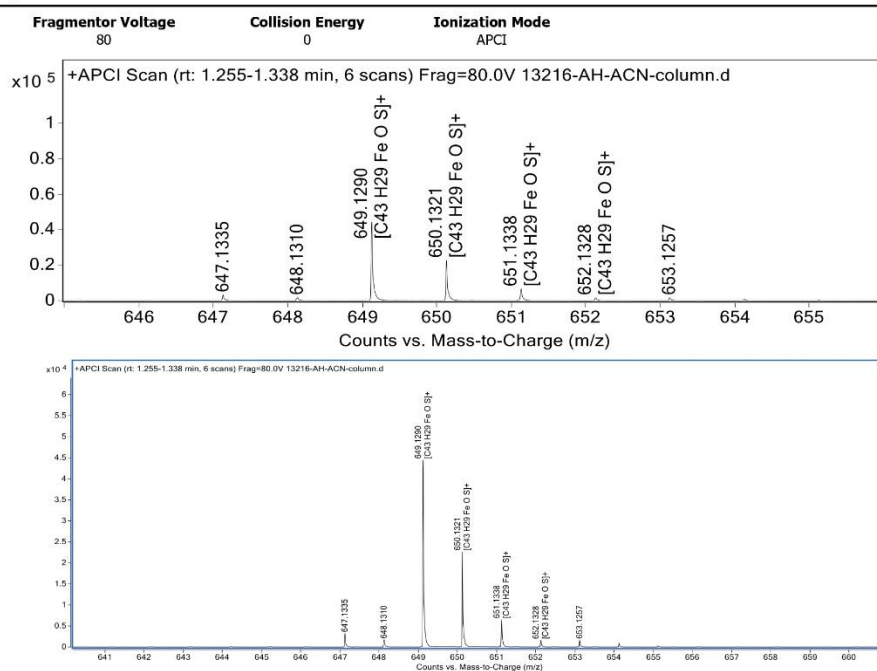


Figure S17. High-resolution APCI-MS spectra of chemically oxidized, irradiated $\text{Fc}_2\text{An}_2\text{SO}$ (range from $m/z = 640$ to 656 shown).

Spectra

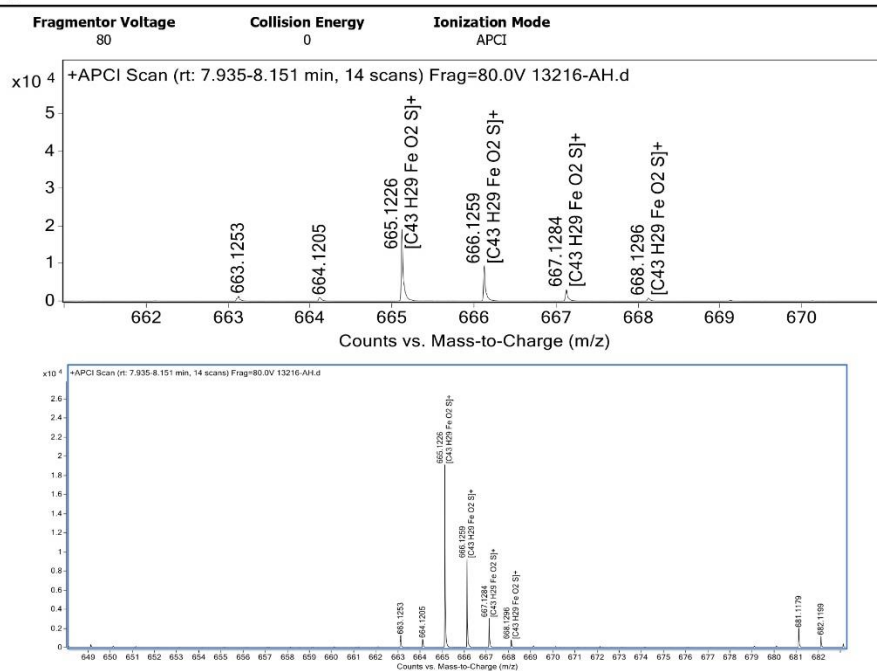


Figure S18. High-resolution APCI-MS spectra of chemically oxidized, irradiated $\text{Fc}_2\text{An}_2\text{SO}$ (range from $m/z = 661$ to 671 shown).

Spectra

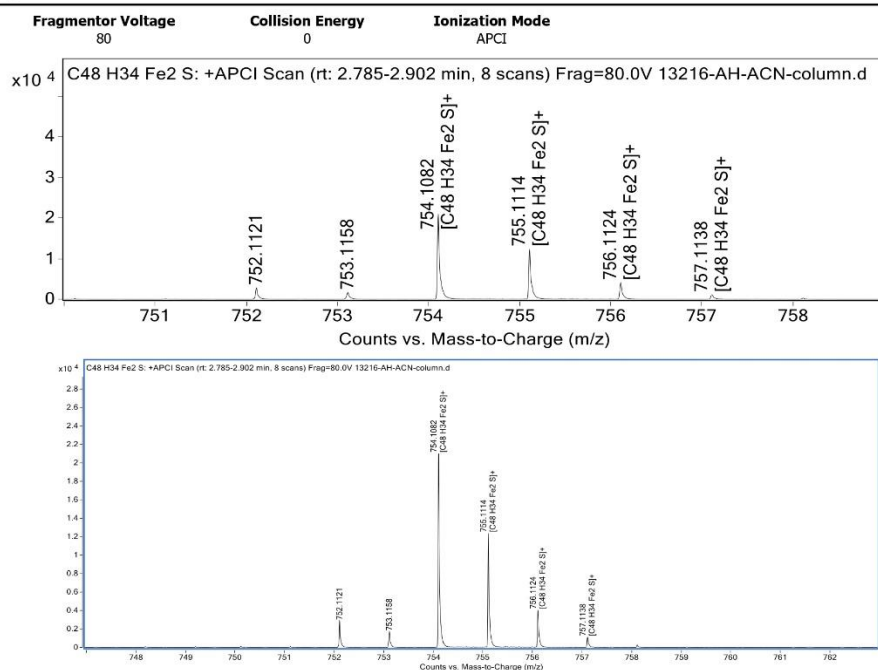


Figure S19. High-resolution APCI-MS spectra of chemically oxidized, irradiated $\text{Fc}_2\text{An}_2\text{SO}$ (range from $m/z = 750$ to 759 shown).

Spectra

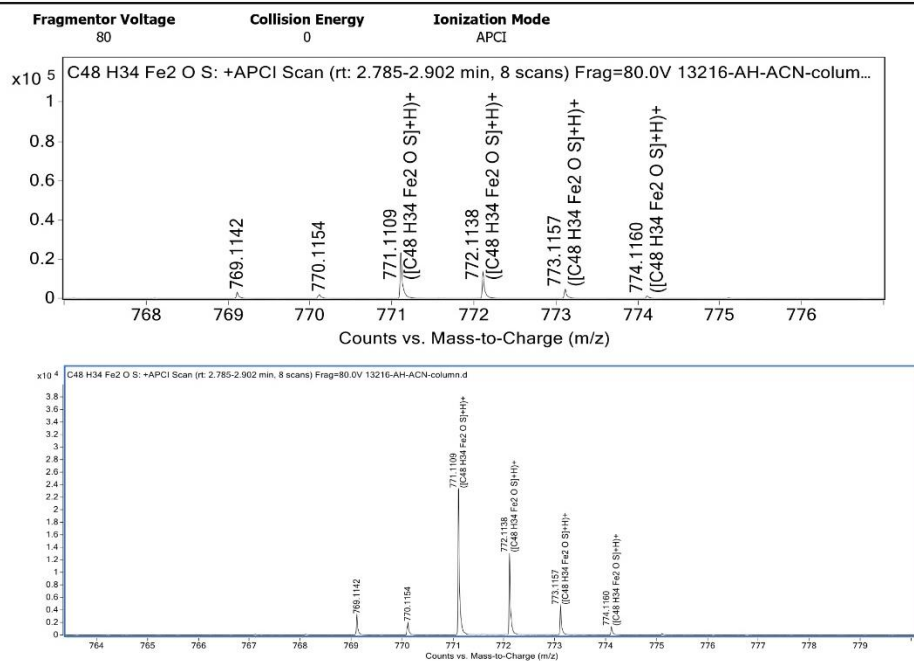


Figure S20. High-resolution APCI-MS spectra of chemically oxidized, irradiated $\text{Fc}_2\text{An}_2\text{SO}$ (range from $m/z = 767$ to 777 shown).

Crystallography

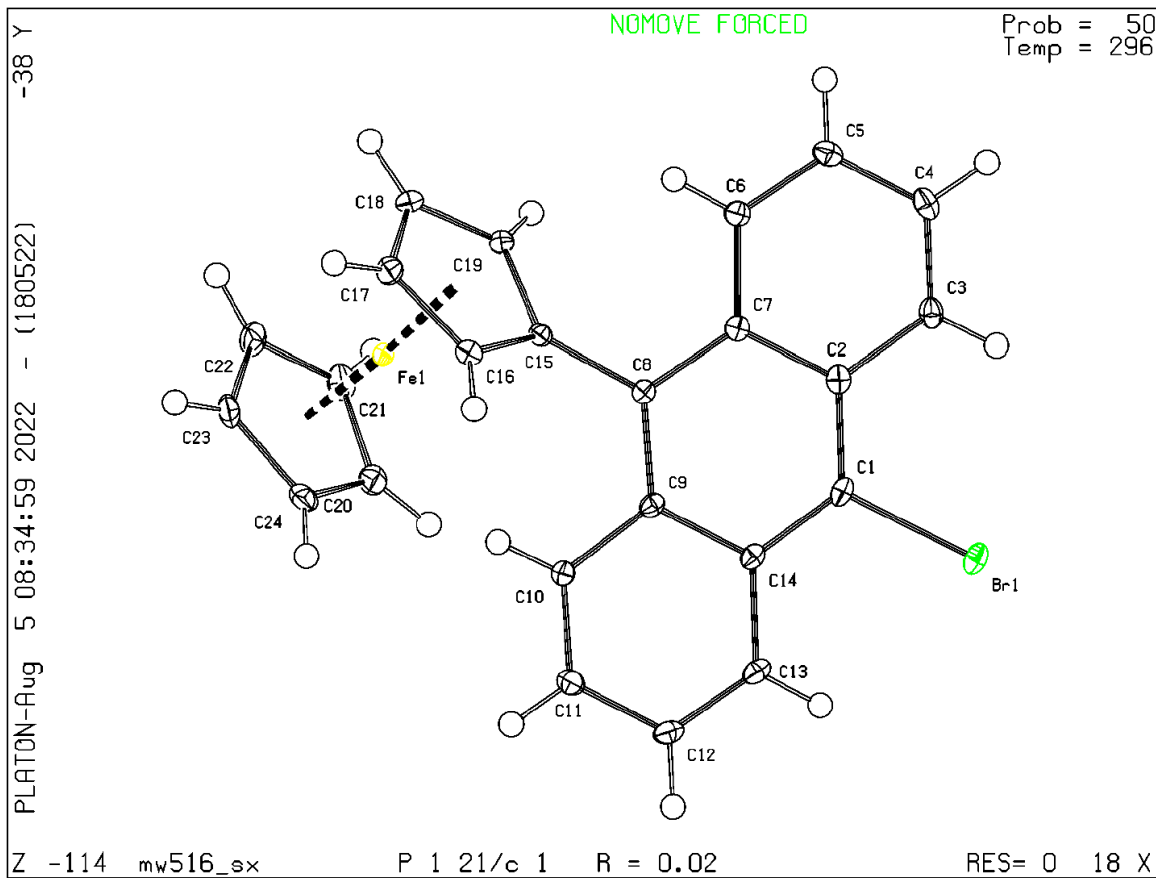


Figure S21. ORTEP of FcAnBr.

Table S1. Crystallographic data and structural refinement for **FcAnBr**.

Empirical formula	C ₂₄ H ₁₇ FeBr
Molecular Weight, g/mol	441.13
Temperature, K	296.15
Crystal system	monoclinic
Space group	P21/c
a, Å	10.024(2)
b, Å	14.043(3)
c, Å	12.112(2)
α , °	90
β , °	97.624(6)
γ , °	90
Volume, Å ³	1689.8(6)
Z	4
ρ_{calc} , cm ³	1.734
μ , mm ⁻¹	3.261
F(000)	888.0
Crystal size, mm ³	0.44 × 0.07 × 0.02
Radiation	MoK α , (λ = 0.71073)
2 θ range for data collection, °	4.1 to 61.102
Index ranges	-14 ≤ h ≤ 14, -20 ≤ k ≤ 18, -17 ≤ l ≤ 17
Reflections collected	47676
Independent reflections	5169 [R _{int} = 0.0416, R _{sigma} = 0.0224]
Data/restraints/parameters	5169/0/235
Goodness-of-fit on F ²	1.038
Final R indexes [I ≥ 2 σ (I)]	R ₁ = 0.0226, wR ₂ = 0.0514
Final R indexes [all data]	R ₁ = 0.0292, wR ₂ = 0.0538
Largest diff. peak/hole, Å ⁻³	0.50/-0.37

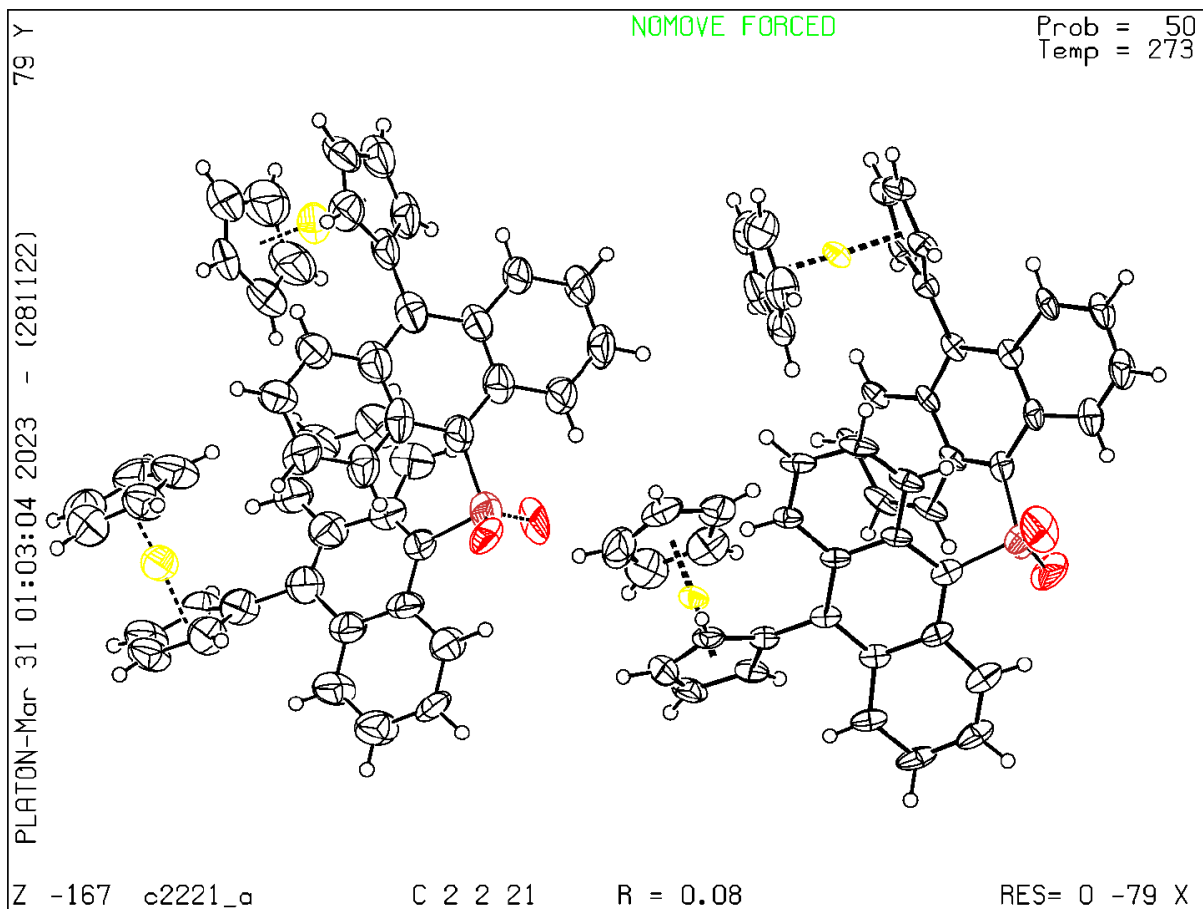


Figure S22. ORTEP of $\text{Fc}_2\text{An}_2\text{SO}$.

Table S2. Crystallographic data and structural refinement for **Fe₂An₂SO**

Empirical formula	C ₄₈ H ₃₄ Fe ₂ OS
Molecular Weight, g/mol	770.51
Temperature, K	273(2)
Crystal system	orthorhombic
Space group	C222 ₁
a, Å	10.591(6)
b, Å	42.48(3)
c, Å	15.387(8)
α, °	90
β, °	90
γ, °	90
Volume, Å ³	6923(7)
Z	8
ρ _{calc} , cm ³	1.479
μ, mm ⁻¹	0.938
F(000)	3184.0
Crystal size, mm ³	0.24 × 0.21 × 0.09
Radiation	MoKα, (λ = 0.71073)
2θ range for data collection, °	1.918 to 48.274
Index ranges	-10 ≤ h ≤ 12, -37 ≤ k ≤ 48, -17 ≤ l ≤ 17
Reflections collected	18005
Independent reflections	5531 [R _{int} = 0.0839, R _{sigma} = 0.0814]
Data/restraints/parameters	5531/1477/632
Goodness-of-fit on F ²	1.093
Final R indexes [I ≥ 2σ (I)]	R ₁ = 0.0776, wR ₂ = 0.1778
Final R indexes [all data]	R ₁ = 0.0979, wR ₂ = 0.1902
Largest diff. peak/hole, Å ⁻³	0.48/-0.50

Electrochemical Data

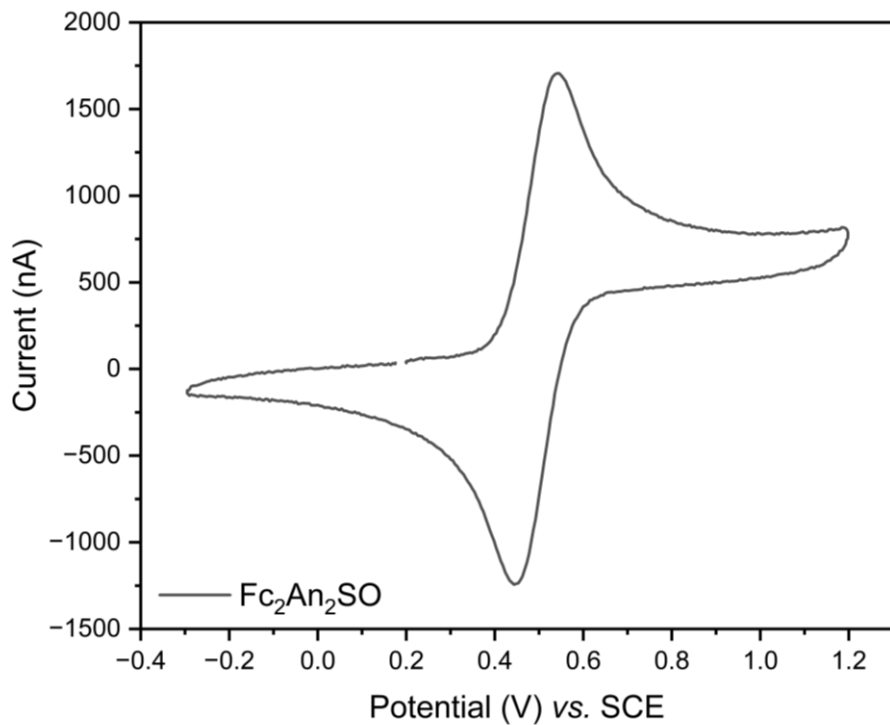


Figure S23. Cyclic voltammogram of $\text{Fc}_2\text{An}_2\text{SO}$ in CH_2Cl_2 (-0.4 V to 1.3 V) with TBAPF_6 electrolyte under nitrogen.

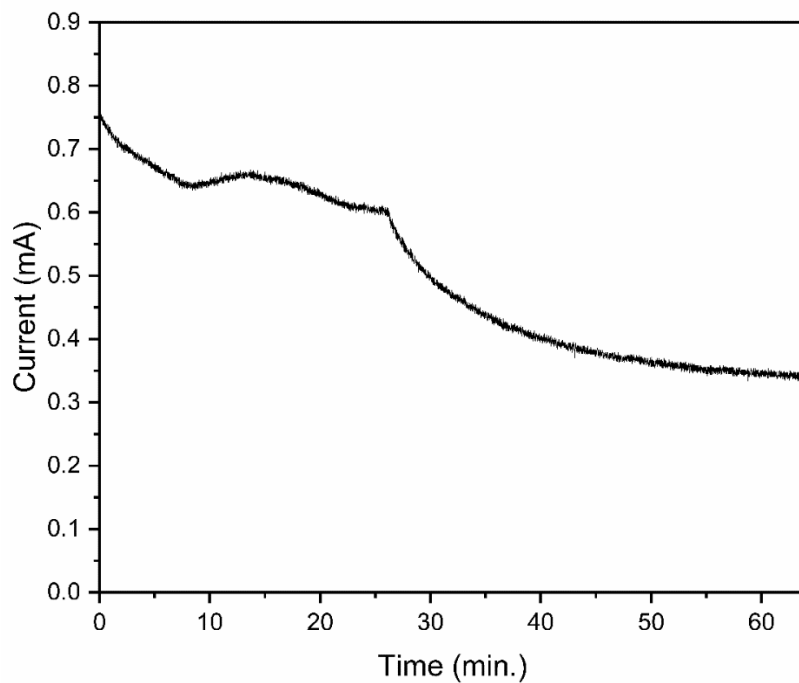


Figure S24. Current vs. time plot for bulk electrolysis of $\text{Fc}_2\text{An}_2\text{SO}$.

Photochemical Data

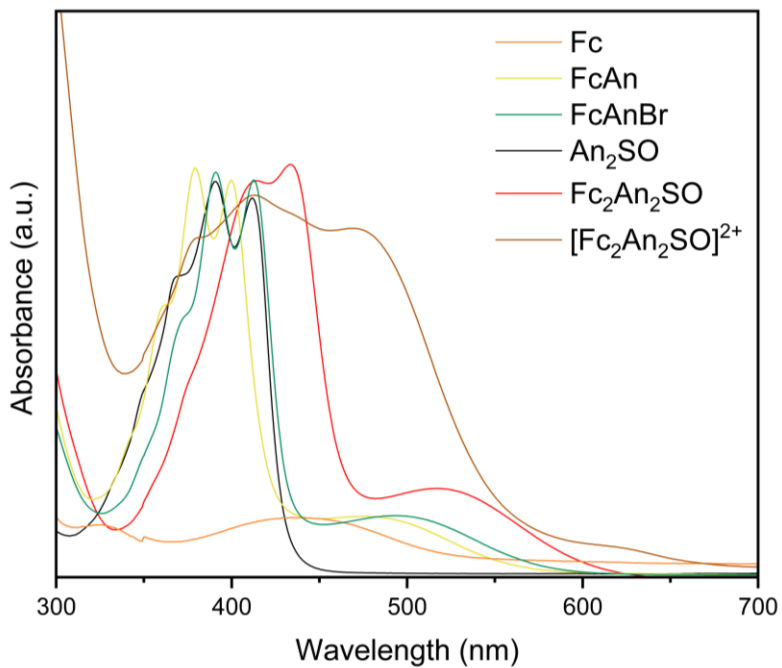


Figure S25. UV/Visible absorption spectra of ferrocene (**Fc**) (orange), ferrocenyl anthracene (**FcAn**) (yellow), 9-bromo-10-ferrocenylanthracene (**FcAnBr**) (green), **An₂SO** (black), **Fc₂An₂SO** (red) and **[Fc₂An₂SO]²⁺** (brown).

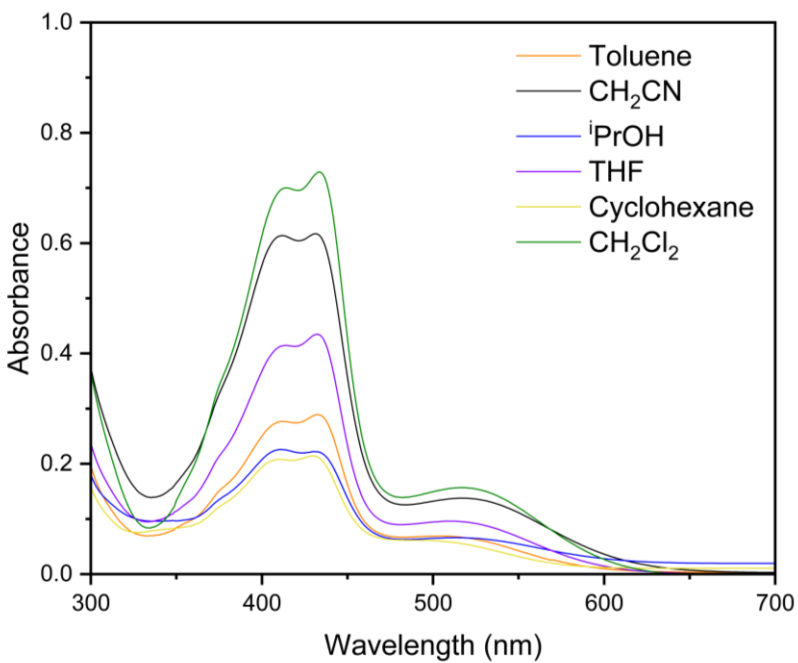


Figure S26. UV/Vis absorption spectra of **Fc₂An₂SO** in different solvents.

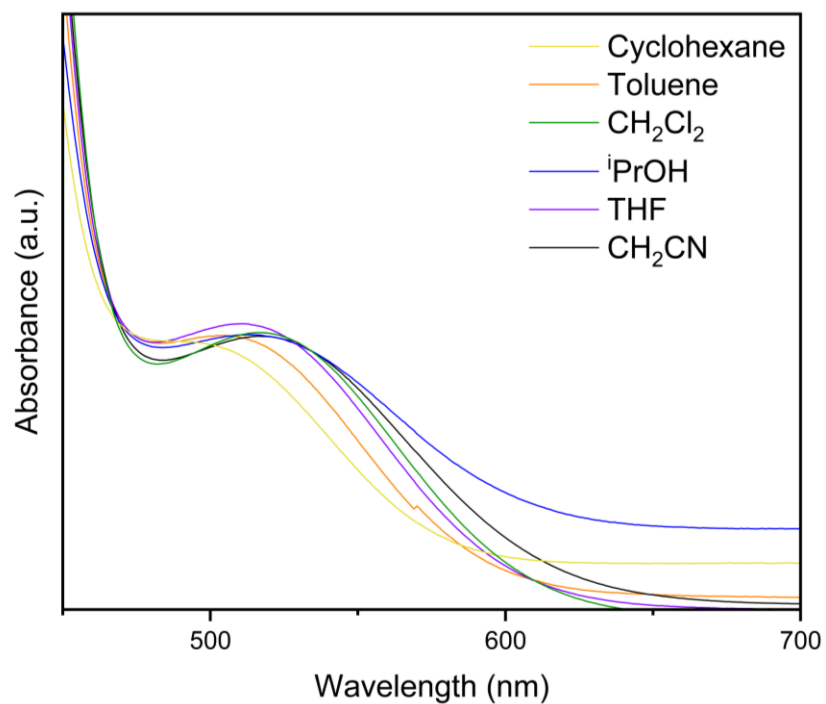


Figure S27. Normalized UV/Vis absorption of $\text{Fc}_2\text{An}_2\text{SO}$ in different solvents (450 nm – 700 nm).

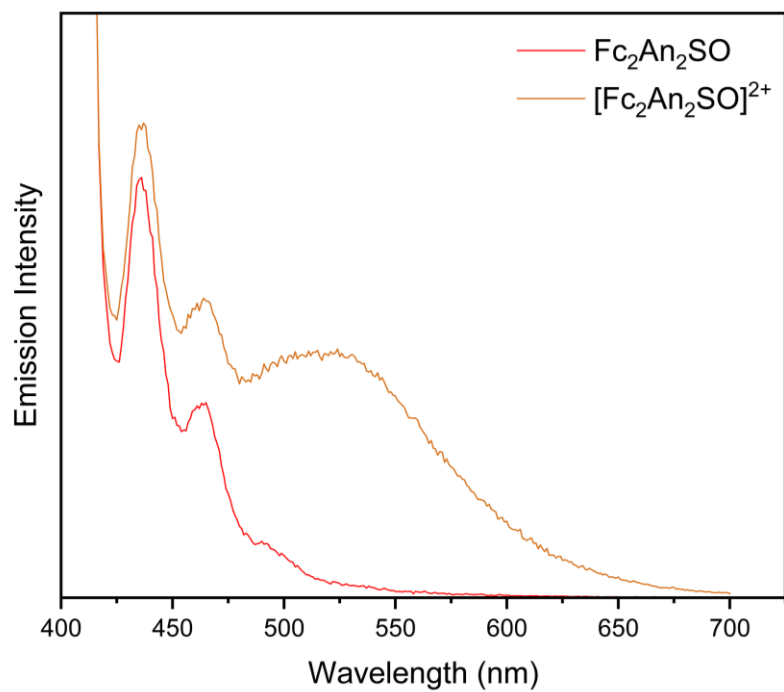


Figure S28. Emission spectra of $\text{Fc}_2\text{An}_2\text{SO}$ (red) and $[\text{Fc}_2\text{An}_2\text{SO}]^{2+}$ (orange).

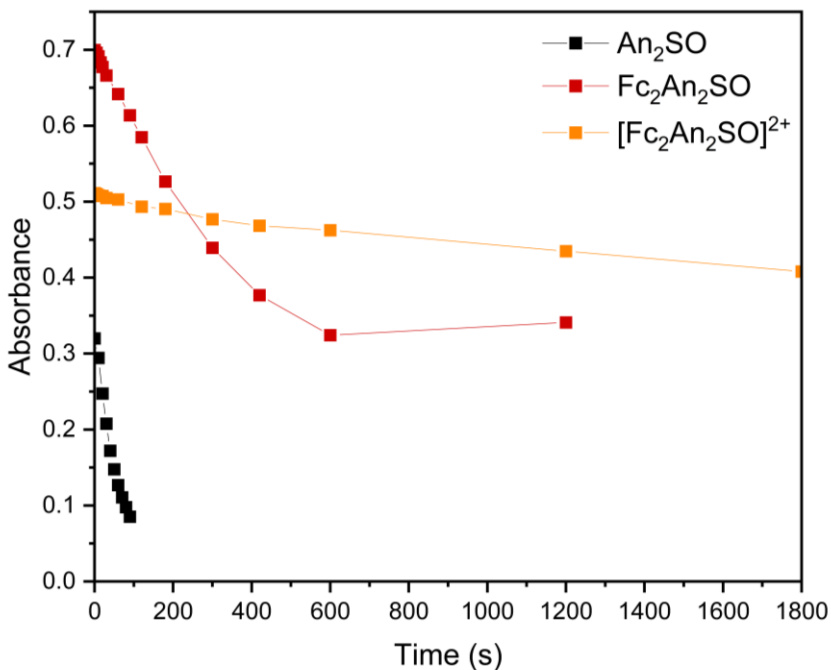


Figure S29. Photochemical rates of reaction of **An₂SO** (black), **Fc₂An₂SO** (red) and **[Fc₂An₂SO]²⁺** (orange). Wavelength of irradiation source (excitation) = 254 nm. Wavelength at which absorption was compared across samples = 413 nm. Time of irradiation; **An₂SO** = 1.5 min, **Fc₂An₂SO** = 20 min, **[Fc₂An₂SO]²⁺** = 30 min.

References

1. O. V. Dolomanov, L. J. Bourhis, R. J. Gildea, J. A. K. Howard, H. Puschmann, *J. Appl. Crystallogr.*, 2009, **42**, 339–341.
2. W. F. Polik, J. R. Schmidt, J. R. *Wiley Interdiscip. Rev. Comput. Mol. Sci.*, 2022, **12**.
3. I. R. Butler, L. J. Hobson, S. J. Coles, M. B. Hursthouse, K. M. Abdul Malik, *J. Organomet. Chem.*, 1997, **540**, 27 – 40.
4. Nikitin, K.; Müller-Bunz, H.; Ortin, Y.; Muldoon, J.; McGlinchey, M. J. *J. Am. Chem. Soc.*, 2010, **132**, 17617–17622.